

1 **Assessment of N95 respirator decontamination and re-use for SARS-CoV-2**

2 Robert J. Fischer¹, Dylan H. Morris², Neeltje van Doremalen¹, Shanda Sarchette¹, M. Jeremiah Matson¹

3 Trenton Bushmaker¹, Claude Kwe Yinda¹, Stephanie N. Seifert¹, Amandine Gamble³, Brandi N.

4 Williamson¹, Seth D. Judson⁴, Emmie de Wit¹, James O. Lloyd-Smith³, Vincent J. Munster¹

5

6 1. National Institute of Allergy and Infectious Diseases, Hamilton, MT

7 2. Princeton University, Princeton, NJ

8 3. University of California, Los Angeles, Los Angeles, CA

9 4. University of Washington, Seattle, WA

10 Dear editor,

11 The unprecedented pandemic of COVID-19 has created worldwide shortages of personal protective
12 equipment, in particular respiratory protection such as N95 respirators(1). SARS-CoV-2 transmission is
13 frequently occurring in hospital settings, with numerous reported cases of nosocomial transmission
14 highlighting the vulnerability of healthcare workers(2). The environmental stability of SARS-CoV-2
15 underscores the need for rapid and effective decontamination methods. In general, N95 respirators are
16 designed for single use prior to disposal. Extensive literature is available for decontamination procedures
17 for N95 respirators, using either bacterial spore inactivation tests, bacteria or respiratory viruses (e.g.
18 influenza A virus)(3-6). Effective inactivation methods for these pathogens and surrogates include UV,
19 ethylene oxide, vaporized hydrogen peroxide (VHP), gamma irradiation, ozone and dry heat(3-7). The
20 filtration efficiency and N95 respirator fit has typically been less well explored, but suggest that both
21 filtration efficiency and N95 respirator fit can be affected by the decontamination method used(7, 8). For
22 a complete list of references see supplemental information.

23
24 Here, we analyzed four different decontamination methods – UV radiation (260 – 285 nm), 70°C dry heat,
25 70% ethanol and vaporized hydrogen peroxide (VHP) – for their ability to reduce contamination with
26 infectious SARS-CoV-2 and their effect on N95 respirator function. For each of the decontamination
27 methods, we compared the normal inactivation rate of SARS-CoV-2 on N95 filter fabric to that on
28 stainless steel, and we used quantitative fit testing to measure the filtration performance of the N95
29 respirators after each decontamination run and 2 hours of wear, for three consecutive decontamination
30 and wear sessions (see supplemental information). VHP and ethanol yielded extremely rapid inactivation
31 both on N95 and on stainless steel (Figure 1A). UV inactivated SARS-CoV-2 rapidly from steel but more
32 slowly on N95 fabric, likely due its porous nature. Heat caused more rapid inactivation on N95 than on
33 steel; inactivation rates on N95 were comparable to UV.

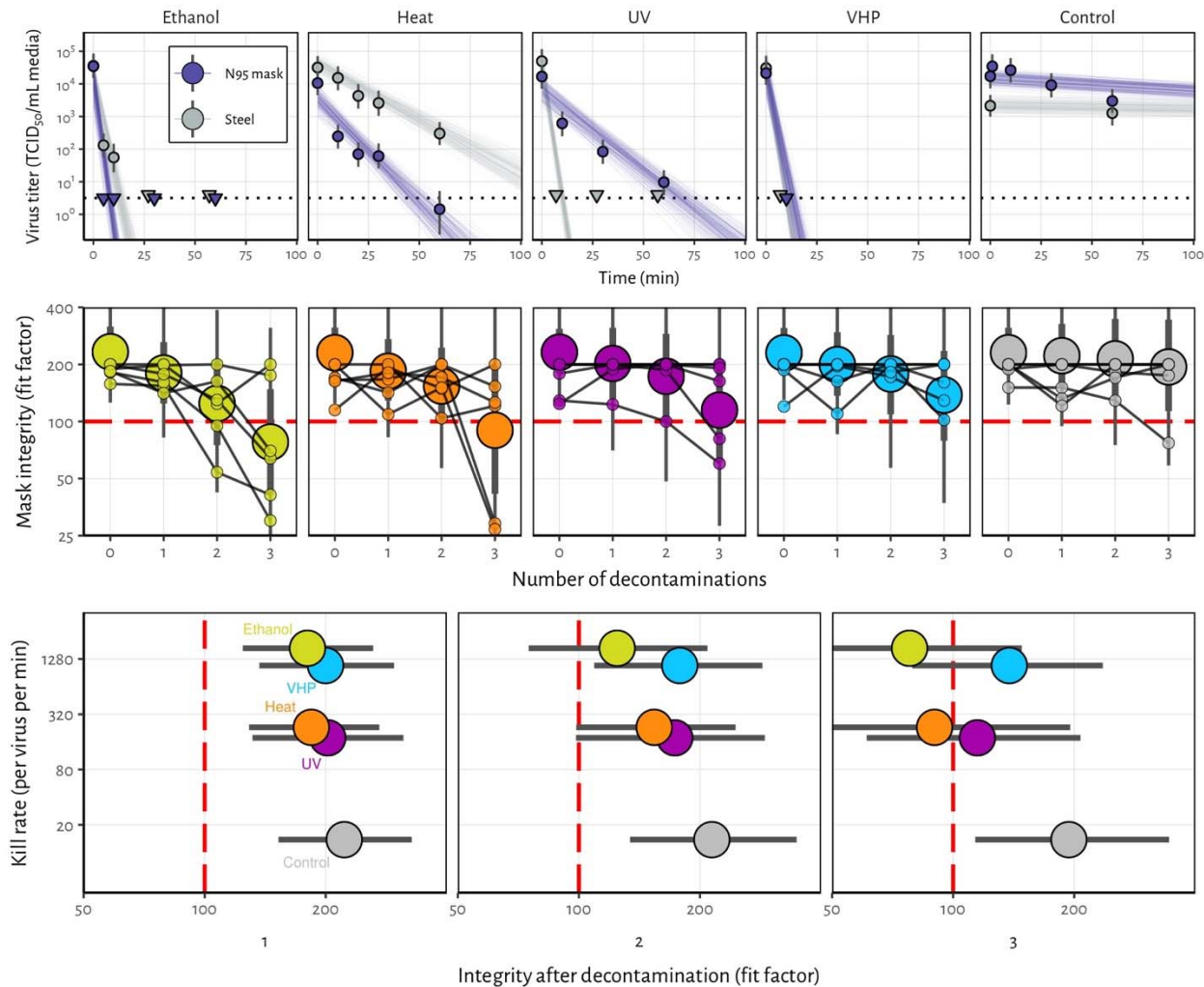
34

35 Quantitative fit tests showed that the filtration performance of the N95 respirator was not markedly
36 reduced after a single decontamination for any of the four decontamination methods (Figure 1B).
37 Subsequent rounds of decontamination caused sharp drops in filtration performance of the ethanol-treated
38 masks, and to a slightly lesser degree, the heat-treated masks. The VHP and UV treated masks retained
39 comparable filtration performance to the control group after two rounds of decontamination, and
40 maintained acceptable performance after three rounds.

41
42 Taken together, our findings show that VHP treatment exhibits the best combination of rapid inactivation
43 of SARS-CoV-2 and preservation of N95 respirator integrity, under the experimental conditions used here
44 (Figure 1C). UV radiation kills the virus more slowly and preserves comparable respirator function. 70°C
45 dry heat kills with similar speed to UV and is likely to maintain acceptable fit scores for two rounds of
46 decontamination. Ethanol decontamination is not recommended due to loss of N95 integrity, echoing
47 earlier findings⁵.

48
49 All treatments, particularly UV and dry heat, should be conducted for long enough to ensure that a
50 sufficient reduction in virus concentration has been achieved. The degree of required reduction will
51 depend upon the degree of initial virus contamination. Policymakers can use our estimated decay rates
52 together with estimates of real-world contamination to choose appropriate treatment durations (see
53 supplemental information).

54
55 Our results indicate that N95 respirators can be decontaminated and re-used in times of shortage for up to
56 three times for UV and HPV, and up to two times for dry heat. However, utmost care should be given to
57 ensure the proper functioning of the N95 respirator after each decontamination using readily available
58 qualitative fit testing tools and to ensure that treatments are carried out for sufficient time to achieve
59 desired risk-reduction. It will therefore be critical that FDA, CDC and OSHA guidelines with regards to
60 fit testing, seal check and respirator re-use are followed(9, 10).



61
 62 **Figure 1.** Decontamination of SARS-CoV-2 by four different methods. **A)** SARS-CoV-2 on N95 fabric
 63 and stainless steel surface was exposed to UV, 70 °C dry heat, 70% ethanol and vaporized hydrogen
 64 peroxide (VHP). 50 μ l of 10⁵ TCID₅₀/mL of SARS-CoV was applied on N95 and stainless steel (SS).
 65 Samples were collected at indicted time-points post exposure to the decontamination method for UV, heat
 66 and ethanol and after 10 minutes for VHP. Viable virus titer is shown in TCID₅₀/mL media on a
 67 logarithmic scale. All samples were quantified by end-point titration on Vero E6 cells. Plots show
 68 estimated mean titer across three replicates (circles and bars show the posterior median estimate of this
 69 mean and a 95% credible interval). Time-points with no positive wells for any replicate are plotted as
 70 triangles at the approximate single-replicate detection limit of the assay (LOD, see Appendix for
 71 discussion) to indicate that a range of sub-LOD values are plausible. Steel points at the LOD are offset

72 slightly up and to the left to avoid overplotting. Lines show predicted decay of virus titer over time (lines;
73 50 random draws per replicate from the joint posterior distribution of the exponential decay rate, i.e.
74 negative of the slope, and intercept, i.e. initial virus titer). Black dotted line shows approximate LOD:
75 $10^{0.5}$ TCID₅₀/mL media. **B) Mask integrity.** Quantitative fit testing results for all the decontamination
76 methods after decontamination and 2 hours of wear, for three consecutive runs. Data from six individual
77 replicates (small dots) for each treatment are shown in addition to an estimated median fit factor (large
78 dots), an estimated 68% range of fit factors (thick bars) and an estimated 95% range (thin bars). Fit
79 factors are a measure of filtration performance: the ratio of the concentration of particles outside the mask
80 to the concentration inside. The measurement machine reports value up to 200. A minimal fit factor of
81 100 (red dashed line) is required for a mask to pass a fit test. **C) SARS-CoV-2 decontamination**
82 performance. Kill rate (y-axis), versus mask integrity after decontamination (x-axis; point represents
83 estimated median, bar length represents estimated 68% range). The three panels report mask integrity
84 after one, two or three decontamination cycles.

85

86 **References**

- 87 1. Ranney ML, Griffeth V, Jha AK. Critical Supply Shortages - The Need for Ventilators and
88 Personal Protective Equipment during the Covid-19 Pandemic. *N Engl J Med.* 2020 Mar 25.
- 89 2. McMichael TM, Currie DW, Clark S, Pogojans S, Kay M, Schwartz NG, et al. Epidemiology of
90 Covid-19 in a Long-Term Care Facility in King County, Washington. *N Engl J Med.* 2020 Mar 27.
- 91 3. Batelle. Final Report for the Bioquell Hydrogen Peroxide Vapor (HPV) Decontamination for Reuse
92 of N95 Respirators. 2016 [cited; Available from: <https://www.fda.gov/media/136386/download>
- 93 4. Fisher EM, Shaffer RE. A method to determine the available UV-C dose for the decontamination
94 of filtering facepiece respirators. *J Appl Microbiol.* 2011 Jan;110(1):287-95.
- 95 5. Heimbuch BK, Wallace WH, Kinney K, Lumley AE, Wu CY, Woo MH, et al. A pandemic influenza
96 preparedness study: use of energetic methods to decontaminate filtering facepiece respirators
97 contaminated with H1N1 aerosols and droplets. *Am J Infect Control.* 2011 Feb;39(1):e1-9.
- 98 6. Lin TH, Tang FC, Hung PC, Hua ZC, Lai CY. Relative survival of *Bacillus subtilis* spores loaded
99 on filtering facepiece respirators after five decontamination methods. *Indoor Air.* 2018 May 31.
- 100 7. Avilash Cramer ET, Sherryl H Yu, Mitchell Galanek, Edward Lamere, Ju Li, Rajiv Gupta, Michael
101 P Short. disposable N95 masks pass qualitative fit-test but have decreases filtration efficiency after
102 cobalt-60 gamma irradiation. *MedRxiv.*
- 103 8. Lin TH, Chen CC, Huang SH, Kuo CW, Lai CY, Lin WY. Filter quality of electret masks in filtering
104 14.6-594 nm aerosol particles: Effects of five decontamination methods. *PLoS One.*
105 2017;12(10):e0186217.
- 106 9. (NIOSH) TNIfOSaH. Decontamination and Reuse of Filtering Facepiece Respirators
107 . 2020 [cited 2020 4/5/2020]; Available from: [https://www.cdc.gov/coronavirus/2019-ncov/hcp/ppe-](https://www.cdc.gov/coronavirus/2019-ncov/hcp/ppe-strategy/decontamination-reuse-respirators.html)
108 [strategy/decontamination-reuse-respirators.html](https://www.cdc.gov/coronavirus/2019-ncov/hcp/ppe-strategy/decontamination-reuse-respirators.html)

109 10. CDC. Recommended Guidance for Extended Use and Limited Reuse of N95 Filtering Facepiece
110 Respirators in Healthcare Settings. 2020 [cited; Available from:
111 <https://www.cdc.gov/niosh/topics/hcwcontrols/recommendedguidanceextuse.html>

112

113

114

115

116

117

118

119

120

121

122

123

124

125

126

127

128

129

130

131

132

133

134

135

136	Table of contents:	page 1
137	Supplemental methods	page 2
138	Supplemental table	page 10
139	Code and data availability	page 10
140	Acknowledgements	page 11
141	Supplemental references	page 11

142 **Supplemental methods**

143 *Short literature review on mask decontamination*

144 The COVID-19 pandemic has highlighted the necessity for large-scale decontamination procedures
145 for personal protective equipment (PPE), in particular N95 respirator masks(1). SARS-CoV-2 has
146 frequently been detected on PPE of healthcare workers(11). The environmental stability of SARS-CoV-2
147 underscores the need for rapid and effective decontamination methods(12). Extensive literature is
148 available for decontamination procedures for N95 respirators, using either bacterial spore inactivation
149 tests, bacteria or respiratory viruses (e.g. influenza A virus)(3-6, 9, 13-15). Effective inactivation methods
150 for these pathogens and surrogates include UV, ethylene oxide, vaporized hydrogen peroxide (VHP),
151 gamma irradiation, ozone and dry heat(4, 5, 7, 9, 14-16). The filtration efficiency and N95 respirator fit
152 has typically been less well explored, but suggest that both filtration efficiency and N95 respirator fit can
153 be affected by the decontamination method used(7, 8). It will therefore be critical that FDA, CDC and
154 OSHA guidelines with regards to fit testing, seal check and respirator re-use are followed(9, 17-20).

155 *Laboratory experiments*

156 Viruses and titration

157 HCoV-19 nCoV-WA1-2020 (MN985325.1) was the SARS-CoV-2 strain used in our
158 comparison(21). Virus was quantified by end-point titration on Vero E6 cells as described previously(22).
159 Virus titrations were performed by end-point titration in Vero E6 cells. Cells were inoculated with 10-fold
160 serial dilutions in four-fold of samples taken from N95 mask and stainless steel surfaces (see below). One
161 hour after inoculation of cells, the inoculum was removed and replaced with 100 μ l (virus titration)
162 DMEM (Sigma-Aldrich) supplemented with 2% fetal bovine serum, 1 mM L-glutamine, 50 U/ml
163 penicillin and 50 μ g/ml streptomycin. Six days after inoculation, cytopathogenic effect was scored and
164 the TCID₅₀ was calculated (see below). Wells presenting cytopathogenic effects due to media toxicity

165 (e.g., due to the presence of ethanol or hydrogen peroxide) rather than viral infection were removed from
166 the titer inference procedure.

167 N95 and stainless steel surface

168 N95 material discs were made by punching 9/16" (15 mm) fabric discs from N95 respirators,
169 AOSafety N9504C respirators (Aearo Company Southbridge, MA). The stainless steel 304 alloy discs
170 were purchased from Metal Remnants (<https://metalremnants.com/>) as described previously. 50 μ L of
171 SARS-CoV-2 was spotted onto each disc. A 0 time-point measurement was taken prior to exposing the
172 discs to the disinfection treatment. At each sampling time-point, discs were rinsed 5 times by passing the
173 medium over the stainless steel or through the N95 disc. The medium was transferred to a vial and frozen
174 at -80°C until titration. All experimental conditions were performed in triplicate.

175 Decontamination methods

176 *Ultraviolet light.* Plates with fabric and steel discs were placed under an LED high power UV germicidal
177 lamp (effective UV wavelength 260-285nm) without the titanium mesh plate (LEDi2, Houston, Tx) 50
178 cm from the UV source. At 50 cm the UVC power was measured by the manufacturer at $550 \mu\text{W}/\text{cm}^2$.
179 Plates were removed at 10, 30 and 60 minutes and 1 mL of cell culture medium added. The energy the
180 discs were exposed to at 10, 30 and 60 min is $0.33 \text{ J}/\text{cm}^2$, $0.99 \text{ J}/\text{cm}^2$, and $1.98 \text{ J}/\text{cm}^2$ respectively. While
181 the CDC has no specific recommendations on the minimum dose, they do report that a $1 \text{ J}/\text{cm}^2$ dose can
182 reduce tested viable viral loads by 99.9%⁴.

183 *Heat treatment.* Plates with fabric and steel discs were placed in a 70°C oven. Plates were removed at 10,
184 20, 30 and 60 minutes and 1 mL of cell culture medium added.

185 *70% ethanol.* Fabric and steel discs were placed into the wells of one 24 well plate per time-point and
186 sprayed with 70% ethanol to saturation. The plate was tipped to near vertical and 5 passes of ethanol were

187 sprayed onto the discs from approximately 10 cm. After 10 minutes, 1 mL of cell culture medium was
188 added.

189 *VHP*. Plates with fabric and steel discs were placed into a Panasonic MCO-19AIC-PT (PHC Corp. of
190 North America Wood Dale, IL) incubator with VHP generation capabilities and exposed to hydrogen
191 peroxide (approximately 1000 ppm). The exposure to VHP was 7 minutes, after the inactivation of the
192 hydrogen peroxide, the plate was removed and 1 mL of cell culture medium was added.

193 *Control*. Plates with fabric and steel discs and steel plates were maintained at 21-23°C and 40% relative
194 humidity for up to four days. After the designated time-points, 1 mL of cell culture medium was added.

195 N95 mask integrity testing

196 N95 Mask (3M™ Aura™ Particulate Respirator 9211+/37193) integrity testing after 2 hours of wear
197 and decontamination, for three consecutive rounds, was performed for a total of 6 times for each
198 decontamination condition and control condition. Masks were worn by subjects and integrity was
199 quantitatively determined using the Portacount Respirator fit tester (TSI, 8038) with the N95 companion
200 component, following the modified ambient aerosol condensation nuclei counter quantitative fit test
201 protocol approved by the OSHA¹⁸. Subjects were asked to bend over for 40 seconds, talk for 50 seconds,
202 move head from side-to-side for 50 seconds, and move head up-and-down for 50 seconds whilst aerosols
203 on inside and outside of mask were measured. By convention, this fit test is passed when the final score is
204 ≥ 100 . For the N95 integrity testing, a Honeywell Mistmate humidifier (cat#HUL520B) was used for
205 particle generation.

206 *Statistical analyses*

207 In the model notation that follows, the symbol \sim denotes that a random variable is distributed
208 according to the given distribution. Normal distributions are parametrized as Normal(mean, standard
209 deviation). Positive-constrained normal distributions (“Half-Normal”) are parametrized as Half-

210 Normal(mode, standard deviation). Normal distributions truncated to the interval [0, 1] are parameterized
211 as TruncNormal(mode, standard deviation).

212 We use $\langle \text{Distribution Name} \rangle \text{CDF}(x \mid \text{parameters})$ and $\langle \text{Distribution Name} \rangle \text{CCDF}$ to denote the
213 cumulative distribution function and complementary cumulative distribution functions of a probability
214 distribution, respectively. So for example $\text{NormalCDF}(5 \mid 0, 1)$ is the value of the $\text{Normal}(0, 1)$
215 cumulative distribution function at 5.

216 We use $\text{logit}(x)$ and $\text{invlogit}(x)$ to denote the logit and inverse logit functions, respectively:

217
$$\text{logit}(x) = \ln \frac{x}{1-x} \quad (1)$$

218
$$\text{invlogit}(x) = \frac{e^x}{1+e^x} \quad (2)$$

219 Mean titer inference

220 We inferred mean titers across sets of replicates using a Bayesian model. The \log_{10} titers v_{ijk} (the titer
221 for the sample from replicate k of time-point j of experiment i) were assumed to be normally distributed
222 about a mean μ_{ij} with a standard deviation σ . We placed a very weakly informative normal prior on the
223 \log_{10} mean titers μ_{ij} :

224
$$\mu_{ij} \sim \text{Normal}(3, 3) \quad (3)$$

225 We placed a weakly informative normal prior on the standard deviation:

226
$$\sigma \sim \text{Normal}(0, 0.5) \quad (4)$$

227 We then modeled individual positive and negative wells for sample ijk according to a Poisson single-
228 hit model(23). That is, the number of virions that successfully infect cells in a given well is Poisson
229 distributed with mean:

230
$$V = \ln(2) 10^v \quad (5)$$

231 where v is the \log_{10} virus titer in TCID₅₀, where v is the \log_{10} virus titer in TCID₅₀, and the well is infected
232 if at least one virion successfully infects a cell. The value of the mean derives from the fact that our units
233 are TCID₅₀; the probability of infection at $v = 0$, i.e. 1 TCID₅₀, is equal to $1 - e^{-\ln(2) \times 1} = 0.5$.

234 Let Y_{ijkl} be a binary variable indicating whether the l^{th} well of dilution factor d (expressed as \log_{10}
235 dilution factor) of sample ijk was positive (so $Y_{ijkl} = 1$ if the well was positive and 0 otherwise), which
236 will occur as long as at least one virion successfully infects a cell.

237 It follows from (5) that the conditional probability of observing $Y_{ijkl} = 1$ given a true underlying titer
238 \log_{10} titer v_{ijk} is given by:

239
$$L(Y_{ijkl} = 1 | v_{ijk}) = 1 - e^{-\ln(2) \times 10^x} \quad (6)$$

240 Where

241
$$x = v_{ijk} - d \quad (7)$$

242 is the expected concentration, measured in \log_{10} TCID₅₀, in the dilute sample. This is simply the
243 probability that a Poisson random variable with mean $(-\ln(2) \times 10^x)$ is greater than 0. Similarly, the
244 conditional probability of observing $Y_{ijkl} = 0$ given a true underlying titer \log_{10} titer v_{ijk} is given by:

245
$$L(Y_{ijkl} = 0 | v_{ijk}) = e^{-\ln(2) \times 10^x} \quad (8)$$

246 which is the probability that the Poisson random variable is 0.

247 This gives us our likelihood function, assuming independence of outcomes across wells.

248 Virus inactivation regression

249 The durations of detectability depend on the decontamination treatment but also initial inoculum and
250 sampling method, as expected. We therefore estimated the decay rates of viable virus titers using a
251 Bayesian regression analogous to that used in van Doremalen et al., 2020(12). This modeling approach
252 allowed us to account for differences in initial inoculum levels across replicates as well as other sources
253 of experimental noise. The model yields estimates of posterior distributions of viral decay rates and half-
254 lives in the various experimental conditions – that is, estimates of the range of plausible values for these
255 parameters given our data, with an estimate of the overall uncertainty(24).

256 Our data consist of 10 experimental conditions: 2 materials (N95 masks and stainless steel) by 5
257 treatments (no treatment, ethanol, heat, UV and VHP). Each has three replicates, and multiple time-points
258 for each replicate. We analyze the two materials separately. For each, we denote by Y_{ijkl} the positive or
259 negative status (see above) for well l which has dilution d for the titer v_{ijk} from experimental condition i
260 during replicate j at time-point k .

261 We model each replicate j for experimental condition i as starting with some true initial \log_{10} titer
262 $v_{ij}(0) = v_{ij0}$. We assume that viruses in experimental condition i decay exponentially at a rate λ_i over time t .
263 It follows that:

264
$$v_{ij}(t) = v_{ij0} - \lambda_i t \quad (9)$$

265 We use the direct-from-well data likelihood function described above, except that now instead of
266 estimating titer distribution about a shared mean μ_{ij} we estimate λ_i under the assumptions that our
267 observed well data Y_{ijkl} reflect the titers $v_{ij}(t)$.

268 *Regression prior distributions*

269 We place a weakly informative Normal prior distribution on the initial \log_{10} titers v_{ij0} to rule out
270 implausibly large or small values (e.g. in this case undetectable \log_{10} titers or \log_{10} titers much higher than
271 the deposited concentration), while allowing the data to determine estimates within plausible ranges:

272
$$v_{ij0} \sim \text{Normal}(4.5, 2) \quad (10)$$

273 We placed a weakly informative Half-Normal prior on the exponential decay rates λ_i :

274
$$\lambda_i \sim \text{Half-Normal}(0.5, 4) \quad (11)$$

275 Our plated samples were of volume 0.1 mL, so inferred titers were incremented by 1 to convert to
276 units of $\log_{10} \text{TCID}_{50}/\text{mL}$.

277 Mask integrity estimation

278 To quantify the decay of mask integrity after repeated decontamination, we used a logit-linear spline
279 Bayesian regression to estimate the rate of degradation of mask fit factors over time, accounting for the
280 fact that fit factors are interval-censored ratios. Fit factors are defined as the ratio of exterior
281 concentration to interior concentration of a test aerosol. They are reported to the nearest integer, up to a
282 maximum readout of 200, but arbitrarily large true fit factors are possible as the mask performance
283 approaches perfect filtration.

284 We had 6 replicate masks j for each of 5 treatments i (no decontamination, ethanol, heat, UV and
285 VHP). Each mask j was assessed for fit factor at 4 time-points k : before decontamination, and then after 1,
286 2, and 3 decontamination cycles. We label the control treatment $i = 0$. So we denote by F_{ijk} the fit factor
287 for the j^{th} mask from the i^{th} treatment after k decontaminations (with $k = 0$ for the initial value).

288 We first converted fit factors F_{ijk} to the equivalent observed filtration rate Y_{ijk} by:

289
$$Y = 1 - 1/F \quad (12)$$

290 *Observation model and likelihood function*

291 We modeled the censored observation process as follows. $\text{logit}(Y_{ijk})$ values are observed with
292 Gaussian error about the true filtration $\text{logit}(p_{ijk})$, with an unknown standard deviation σ_o , and then
293 converted to fit factors, which are then censored:

$$294 \quad \text{logit}(Y_{ijk}) \sim \text{Normal}(\text{logit}(p_{ijk}), \sigma_o) \quad (13)$$

295 Because our reported fit factors are known to be within integer values and right-censored at 200, for
296 $F_{ijk} \geq 200$ we have a conditional probability of observing the data given the parameters of

$$297 \quad L(F_{ijk} | p_{ijk}, \sigma_o) = \text{NormalCCDF}(\text{logit}(1 - 1/200) | \text{logit}(p_{ijk}) \sigma_o) \quad (14)$$

298 That is, we calculate the probability of observing a value of F greater than or equal to 200 (equivalent a
299 value of Y greater than or equal to $1 - 1/200$), given our parameters.

300 For $1.5 \leq F_{ijk} < 200$, we first calculate the upper and lower bounds of our observation $Y^+_{ijk} = 1 - 1 /$
301 $(F_{ijk} - 0.5)$ and $Y^-_{ijk} = 1 - 1 / (F_{ijk} - 0.5)$. Then:

$$302 \quad L(F_{ijk} | p_{ijk}, \sigma_o) = \text{NormalCDF}(\text{logit}(Y^+_{ijk}) | \text{logit}(p_{ijk}) \sigma_o) - \\ 303 \quad \text{NormalCDF}(\text{logit}(Y^-_{ijk}) | \text{logit}(p_{ijk}) \sigma_o) \quad (15)$$

304 That is, we calculate the probability of observing a value between Y^+_{ijk} and Y^-_{ijk} , given our parameters.

305 *Decay model*

306 We assumed that each mask had some true initial filtration rate p_{ij0} . We assumed that these were
307 logit-normally distributed about some unknown mean mask initial filtration rate p_{avg} with a standard
308 deviation σ_p , that is:

309
$$\text{logit}(p_{ij0}) \sim \text{Normal}(\text{logit}(p_{avg}), \sigma_p) \quad (16)$$

310 We then assumed that the logit of the filtration rate, $\text{logit}(p_{ijk})$, decreased after each decontamination
311 by a quantity $d_{0k} + d_{ik}$, where d_{0k} is natural degradation during the k^{th} trial in the absence of
312 decontamination (i.e. the degradation rate in the control treatment, $i = 0$), and d_{ik} is the additional
313 degrading effect of the k^{th} decontamination treatment of type $i > 0$). So for $k = 1, 2, 3$ and $i > 0$:

314
$$\text{logit}(p_{ijk}) = \text{logit}(p_{ij(k-1)}) - (d_{0k} + d_{ik}) + \varepsilon_{ijk} \quad (17)$$

315 where ε_{ijk} is a normally-distributed error term with an inferred standard deviation $\sigma_{\varepsilon_{ijk}}$ for each treatment
316 and decontamination level.

317
$$\varepsilon_{ijk} \sim \text{Normal}(0, \sigma_{\varepsilon_{ijk}}) \quad (18)$$

318 And for the control $i = 0$:

319
$$\text{logit}(p_{0jk}) = \text{logit}(p_{0j(k-1)}) - d_{0k} + \varepsilon_{0jk} \quad (19)$$

320 *Model prior distributions*

321 We placed a weakly informative Half-Normal prior on the control degradation rate d_0 :

322
$$d_0 \sim \text{Half-Normal}(0, 0.5) \quad (20)$$

323 We placed a weakly informative Half-Normal prior on the non-control degradation rates $d_i, i > 0$:

324
$$d_i \sim \text{Half-Normal}(0.25, 0.5) \quad (21)$$

325 reflecting the conservative assumption that decontamination should degrade the mask at least somewhat.

326 We placed a Truncated Normal prior on the mean initial filtration p_{avg} :

327
$$p_{avg} \sim \text{TruncNormal}(0.995, 0.02) \quad (22)$$

328 The mode of 0.995 corresponds to the maximum measurable fit factor of 200. The standard deviation of
329 0.02 leaves it plausible that some masks could start near or below the minimum acceptable threshold fit
330 factor of 100, which corresponds to a p of 0.99.

331 We placed weakly informative Half-Normal priors on the logit-space standard deviations σ_p , σ_{eik} , and
332 σ_o . σ_p reflects variation in individual masks' initial filtration about p_{avg} . The various σ_{eik} reflect variation in
333 masks' true degree of degradation between decontaminations about the expected degree of decay, and σ_o
334 reflects noise in the observation process.

335
$$\sigma_p, \sigma_o \sim \text{Half-Normal}(0, 0.5)$$

336 (23)

337
$$\sigma_{eik} \sim \text{Half-Normal}(0, 0.33)$$

338 We chose standard deviations less than or equal to 0.5 for these normal hyperpriors because a
339 standard deviation of 1.5 (i.e. 3σ in the hyperprior) in logit space corresponds to probability values being
340 uniformly distributed between 0 and 1; we therefore wish to tell our model not to use larger values of σ_p ,
341 σ_o , or σ_{eik} , as these would squash all p_{ijk} to one of two modes, one at 0 and one at 1(25).

342 Markov Chain Monte Carlo Methods

343 For all Bayesian models, we drew posterior samples using Stan (Stan Core Team 2018), which
344 implements a No-U-Turn Sampler (a form of Markov Chain Monte Carlo), via its R interface RStan. We
345 ran four replicate chains from random initial conditions for 2000 iterations, with the first 1000 iterations
346 as a warmup/adaptation period. We saved the final 1000 iterations from each chain, giving us a total of
347 4000 posterior samples. We assessed convergence by inspecting trace plots and examining R^2 and
348 effective sample size (n_{eff}) statistics.

349 Limit of detection (LOD)

350 End-point titration has an approximate limit of detection set by the volume of the undilute sample
351 deposited in each well. If all wells – including those containing undiluted sample – are negative and a
352 Poisson single-hit model is used, the best guess is that the true titer lies somewhere below $1 \text{ TCID}_{50} /$
353 (volume of deposited sample). How far below is determined by the number of wells. For four wells, as
354 was standard in our experiments, the first quarter \log_{10} titer at which 0 wells is the most likely outcome is
355 $10^{-0.5} \text{ TCID}_{50}$ per volume of sample. This is also the imputed Spearman-Kärber titer in that case. Since we
356 used samples of volume 0.1 mL, this corresponds to a value of $10^{0.5} \text{ TCID}_{50}/\text{mL}$. So although we do not
357 use the Spearman-Kärber method here (since we infer mean titers directly from the well data) we use that
358 LOD value to plot samples for which no replicate had a positive well (since the posterior distribution in
359 that case covers a wide-range of sub-threshold values).

360 **Supplemental table**

361 Table S1. Effect of decontamination method on SARS-CoV-2 viability. Results are reported as the
362 median and upper- and lower-limits of the 95% credible interval of the estimated half-life, and time
363 needed to reduce viable SARS-CoV-2 load by a factor of one thousand or one million, based on the
364 posterior distribution of the exponential decay rate of the virus on different materials following different
365 decontamination treatments.

Treatment	Material	Half-life (min)			Time to one thousandth (min)			Time to one millionth (min)		
		Median	2.5%	97.5%	Median	2.5%	97.5%	Median	2.5%	97.5%
Control	N95 mask	78.7	66.1	90.4	784	659	901	1.57×10^3	1.32×10^3	1.8×10^3
	Steel	290	244	327	2.89×10^3	2.43×10^3	3.26×10^3	5.77×10^3	4.86×10^3	6.53×10^3
Ethanol	N95 mask	0.647	0.557	0.733	6.45	5.55	7.31	12.9	11.1	14.6
	Steel	1.08	0.895	1.26	10.8	8.92	12.5	21.6	17.8	23.1
Heat	N95 mask	4.7	3.93	5.48	46.9	39.2	54.6	93.7	78.4	109
	Steel	8.85	7.42	10.2	88.1	74	101	176	148	201
UV	N95 mask	6.12	5.27	6.87	61	52.6	68.5	122	105	137
	Steel	0.736	0.651	0.805	7.33	6.48	8.02	14.7	13	16.6
VHP	N95 mask	0.999	0.83	1.14	9.95	8.27	11.3	19.9	16.5	22.7

Steel		0.77	0.673	0.846		7.67	6.71	8.43		15.3	13.4	16.9
-------	--	------	-------	-------	--	------	------	------	--	------	------	------

366

367

368 **Code and data availability**

369 Code and data to reproduce the Bayesian estimation results and produce corresponding figures are
370 archived online at OSF: <https://doi.org/10.17605/OSF.IO/mkg9b> and available on Github:
371 <https://github.com/dylanmorrison/n95-decontamination>

372 **Acknowledgements**

373 We would like to thank Madison Hebner, Julia Port, Kimberly Meade-White, Irene Offei Owusu,
374 Victoria Avanzato and Lizzette Perez-Perez for excellent technical assistance. This research was
375 supported by the Intramural Research Program of the National Institute of Allergy and Infectious
376 Diseases (NIAID), National Institutes of Health (NIH). JOL-S and AG were supported by the Defense
377 Advanced Research Projects Agency DARPA PREEMPT # D18AC00031 and the UCLA AIDS Institute
378 and Charity Treks, and JOL-S was supported by the U.S. National Science Foundation (DEB-1557022),
379 the Strategic Environmental Research and Development Program (SERDP, RC□2635) of the U.S.
380 Department of Defense. Names of specific vendors, manufacturers, or products are included for public
381 health and informational purposes; inclusion does not imply endorsement of the vendors, manufacturers,
382 or products by the US Department of Health and Human Services.

383 **Supplemental references**

- 384 1. Ranney ML, Griffeth V, Jha AK. Critical Supply Shortages - The Need for Ventilators and
385 Personal Protective Equipment during the Covid-19 Pandemic. *N Engl J Med*. 2020 Mar 25.
- 386 2. McMichael TM, Currie DW, Clark S, Pogosjans S, Kay M, Schwartz NG, et al. Epidemiology of
387 Covid-19 in a Long-Term Care Facility in King County, Washington. *N Engl J Med*. 2020 Mar 27.
- 388 3. Batelle. Final Report for the Bioquell Hydrogen Peroxide Vapor (HPV) Decontamination for Reuse
389 of N95 Respirators. 2016 [cited; Available from: <https://www.fda.gov/media/136386/download>
- 390 4. Fisher EM, Shaffer RE. A method to determine the available UV-C dose for the decontamination
391 of filtering facepiece respirators. *J Appl Microbiol*. 2011 Jan;110(1):287-95.
- 392 5. Heimbuch BK, Wallace WH, Kinney K, Lumley AE, Wu CY, Woo MH, et al. A pandemic influenza
393 preparedness study: use of energetic methods to decontaminate filtering facepiece respirators
394 contaminated with H1N1 aerosols and droplets. *Am J Infect Control*. 2011 Feb;39(1):e1-9.
- 395 6. Lin TH, Tang FC, Hung PC, Hua ZC, Lai CY. Relative survival of *Bacillus subtilis* spores loaded
396 on filtering facepiece respirators after five decontamination methods. *Indoor Air*. 2018 May 31.

- 397 7. Avilash Cramer ET, Sherryl H Yu, Mitchell Galanek, Edward Lamere, Ju Li, Rajiv Gupta, Michael
398 P Short. disposable N95 masks pass qualitative fit-test but have decreases filtration efficiency after
399 cobalt-60 gamma irradiation. MedRxiv.
- 400 8. Lin TH, Chen CC, Huang SH, Kuo CW, Lai CY, Lin WY. Filter quality of electret masks in filtering
401 14.6-594 nm aerosol particles: Effects of five decontamination methods. PLoS One.
402 2017;12(10):e0186217.
- 403 9. (NIOSH) TNIfOSaH. Decontamination and Reuse of Filtering Facepiece Respirators
404 . 2020 [cited 2020 4/5/2020]; Available from: [https://www.cdc.gov/coronavirus/2019-ncov/hcp/ppe-](https://www.cdc.gov/coronavirus/2019-ncov/hcp/ppe-strategy/decontamination-reuse-respirators.html)
405 [strategy/decontamination-reuse-respirators.html](https://www.cdc.gov/coronavirus/2019-ncov/hcp/ppe-strategy/decontamination-reuse-respirators.html)
- 406 10. CDC. Recommended Guidance for Extended Use and Limited Reuse of N95 Filtering Facepiece
407 Respirators in Healthcare Settings. 2020 [cited; Available from:
408 <https://www.cdc.gov/niosh/topics/hcwcontrols/recommendedguidanceextuse.html>
- 409 11. Ong SWX, Tan YK, Chia PY, Lee TH, Ng OT, Wong MSY, et al. Air, Surface Environmental, and
410 Personal Protective Equipment Contamination by Severe Acute Respiratory Syndrome Coronavirus 2
411 (SARS-CoV-2) From a Symptomatic Patient. JAMA. 2020 Mar 4.
- 412 12. van Doremalen N, Bushmaker T, Morris DH, Holbrook MG, Gamble A, Williamson BN, et al.
413 Aerosol and Surface Stability of SARS-CoV-2 as Compared with SARS-CoV-1. N Engl J Med. 2020 Mar
414 17.
- 415 13. Heimbuch BK, Kinney K, Lumley AE, Harnish DA, Bergman M, Wander JD. Cleaning of filtering
416 facepiece respirators contaminated with mucin and Staphylococcus aureus. Am J Infect Control. 2014
417 Mar;42(3):265-70.
- 418 14. Mills D, Harnish DA, Lawrence C, Sandoval-Powers M, Heimbuch BK. Ultraviolet germicidal
419 irradiation of influenza-contaminated N95 filtering facepiece respirators. Am J Infect Control. 2018
420 Jul;46(7):e49-e55.
- 421 15. Viscusi DJ, Bergman MS, Eimer BC, Shaffer RE. Evaluation of five decontamination methods for
422 filtering facepiece respirators. Ann Occup Hyg. 2009 Nov;53(8):815-27.

- 423 16. CDC. Chemical Disinfectants, Guideline for Disinfection and Sterilization in Healthcare Facilities.
424 2008 [cited; Available from: [https://www.cdc.gov/infectioncontrol/guidelines/disinfection/disinfection-
426 methods/chemical.html#Hydrogen](https://www.cdc.gov/infectioncontrol/guidelines/disinfection/disinfection-
425 methods/chemical.html#Hydrogen)
427 17. FDA. N95 Respirators and Surgical Masks (Face Masks). 2020 [cited 2020 4/5/2020]; Available
428 from: [https://www.fda.gov/medical-devices/personal-protective-equipment-infection-control/n95-
430 respirators-and-surgical-masks-face-masks](https://www.fda.gov/medical-devices/personal-protective-equipment-infection-control/n95-
429 respirators-and-surgical-masks-face-masks)
431 18. Administration OSaH. Temporary Enforcement Guidance - Healthcare Respiratory Protection
432 Annual Fit-Testing for N95 Filtering Facepieces During the COVID-19 Outbreak. 2020 [cited; Available
433 from: [https://www.osha.gov/memos/2020-03-14/temporary-enforcement-guidance-healthcare-respiratory-
435 protection-annual-fit](https://www.osha.gov/memos/2020-03-14/temporary-enforcement-guidance-healthcare-respiratory-
434 protection-annual-fit)
436 19. Administration OSaH. User Seal Check Procedures (Mandatory). 2020 [cited 2020 April 11];
437 Available from: <https://www.osha.gov/laws-regs/regulations/standardnumber/1910/1910.134AppB1>
438 20. Administration OSaH. Respirator Fit Testing [WWW Document]. U. S. Dep. Labo. 2012 [cited;
439 Available from: https://www.osha.gov/video/respiratory_protection/fittesting_transcript.html (accessed
440 4.10.20).
441 21. Holshue ML, DeBolt C, Lindquist S, Lofy KH, Wiesman J, Bruce H, et al. First Case of 2019 Novel
442 Coronavirus in the United States. N Engl J Med. 2020 Jan 31.
443 22. van Doremalen N, Bushmaker T, Munster VJ. Stability of Middle East respiratory syndrome
444 coronavirus (MERS-CoV) under different environmental conditions. Euro Surveill. 2013 Sep 19;18(38).
445 23. Brownie C, Statt J, Bauman P, Buczynski G, Skjolaas K, Lee D, et al. Estimating viral titres in
446 solutions with low viral loads. Biologicals. 2011 Jul;39(4):224-30.
447 24. Gelman A. Bayesian data analysis. Third edition. ed. Boca Raton: CRC Press; 2014.
448 25. Northrup JM, Gerber BD. A comment on priors for Bayesian occupancy models. PLoS One.
2018;13(2):e0192819.